Int. J. Electrochem. Sci., 8 **(2013)** 3160 - 3175

International Journal of
ELECTROCHEMICAL
SCIENCE
www.electrochemsci.org

Effects of Heat-Treatment and Pyridine Addition on the Catalytic Activity of Carbon-Supported Cobalt-Phthalocyanine for Oxygen Reduction Reaction in Alkaline Electrolyte

Xianfeng Dai[1], *Jinli Qiao*[1,*], *Xuejun Zhou*[1], *Jingjing Shi*[1], *Pan Xu*[1], *Lei Zhang*[2], *Jiujiun Zhang*[2]

[1]College of Environmental Science and Engineering, Donghua University, 2999 Ren'min North Road, Shanghai 201620, P. R. China
[2] NRC Energy, Mining & Environment, National Research Council of Canada, 4250 Wesbrook Mall, Vancouver, B.C. V6T 1W5
[*]E-mail: qiaojl@dhu.edu.cn

Received: 2 January 2013 / *Accepted:* 5 February 2013 / *Published:* 1 March 2013

Carbon-supported non-precious metal (cobalt) catalysts, namely Py-CoPc/C, where Py is the pyridine and Pc is the phthalocyanine, are synthesized for oxygen reduction reaction (ORR) using combined solvent-impregnation and high-temperature treatment process. The heat-treatment effect on the catalysts' activity toward ORR is examined using catalysts obtained at 600, 700, 800, and 900^{o}C, respectively. The effect of pyridine addition on the ORR activity is also studied. It is found that the formed Py-CoPc/C catalysts all show the higher ORR activities than that of CoPc/C catalyst, and the catalyst obtained at 700^{o}C treatment gives the best activity for the ORR in 0.1M KOH solution, which are tested using both CV and RDE techniques. XRD, TEM as well as XPS are employed to study the crystal structures, morphologies and surface structure changes of the synthesized Py-CoPc/C catalysts. Both XRD and TEM analysis indicate the formation of different amounts of Co-N_X-C active site at different heat-treatment temperatures, which is well correlated with the catalysts' ORR activities. XPS results suggest that the pyridinic-N and graphitic-N groups are both responsible for the enhanced ORR activity, and the catalyst formed at 700^{o}C treatment shows the most amount of these two groups, leading to the most active ORR catalyst.

Keywords: Cobalt-phthalocyanine; pyridine doping; oxygen reduction reaction; heat-treatment; alkaline fuel cell

1. INTRODUCTION

The oxygen reduction reaction (ORR) at the cathode of polymer electrolyte membrane fuel cells (PEMFCs) has been identified as the kinetically dominating reaction when compared to the

hydrogen oxidation reaction (HOR) at the anode. This is because the ORR has a much larger overpotential (or polarization) than that of HOR. Even in an alkaline PEMFC, in which ORR is relatively faster than that in an acidic PEMFC, the kinetics of ORR is still much slower than that HOR. At current technology state, to make PEMFC technically feasible and practical, Pt-based catalysts must be used to catalyze the slow ORR. However, from a consideration of commercialization, the high cost and limited availability of the Pt have been identified as the major barrier [1]. Therefore, exploring low-cost non-precious metal alternatives, such as non-pyrolyzed and pyrolyzed transition metal nitrogen-containing complexes, conductive polymer-based catalysts, transition metal chalcogenides, metal oxides/carbides /nitrides and macrocyclic complexes enzymatic and compounds, have been attracting great attention in the most recent years [2-11]. Among these catalysts, pyrolyzed transition metal N_4-macrocycles (M-N_4-macrocycles) including Fe- or Co-porphyrins and phthalocyanines seem to be the promising catalyst to replace the Pt for the ORR in fuel cell technologies [12-14].

Regarding these M-N_4-macrocycles, after Jasinski [15] discovered the electrocatalytic activity of Co-phthalocyanine (CoPc) for the ORR in alkaline media, Co- and Fe- complexes with phthalocyanines (Pc) or similar N-macrocycles, supported on carbon blacks, have been largely explored as electrocatalysts for the ORR. However, compared to Pt-based catalysts for practical application in fuel cells, both the ORR activity and stability of these transition metal macrocycle catalysts have to be significantly improved. Although a broad range of methodologies and materials have been employed to produce active non-precious metal ORR catalysts, there are still difficulties in discerning the controlling parameters in preparing active catalysts. There is a general agreement in the literature that three necessary factors must co-exist for obtaining the active sites of a catalyst, which are carbon support, a source of transition metal and nitrogen, and pyrolysis (or heat-treatment) [[16]. Among these three factors, heat-treatment seems to play a very important role to improve both the electrocatalytic activity and stability. It was speculated that the chelate polymerization and the adsorbed macrocycle could form several bonds with the carbon support during the heat-treatment, which then facilitated the electron transfer from the carbon support to O_2 [17-21]. Besides heat-treatment, nitrogen sources also have a significant effect on the ORR activity. For example, Wang *et al* [22] reported that more nitrogen addition in the catalyst synthesis could benefit the catalyst's ORR activity. Therefore, in order to improve catalytic activity and stability, we can use nitrogen-containing ligands to modify the transition metal macrocycles.

As a continuing effort in improving carbon supported CoPc catalyst's ORR activity in alkaline solution, in this paper, we added pyridine (Py) into the synthesis precursor containing both CoPc and carbon support, and synthesized a heat-treated catalyst (expressed as Py-CoPc/C) which showed much better ORR activity than those only containing Pc or Py coordinator (CoPc/C or Py-Co/C). The effect of heat-treatment temperature on the electrocatalytic activity of Py-CoPc/C catalysts for the ORR was characterized by cyclic voltammogram (CV) and linear sweep voltammetry (LSV) using rotating disk electrode (RDE) technique. For fundamental understanding, X-ray diffraction (XRD), transmission

electron microscopy (TEM) as well as X-ray photoelectron spectroscopy (XPS) were also used to study the crystal structure, morphology and surface structure changes.

2. EXPERIMENTAL

2.1 Materials and catalyst preparation

Cobalt phthalocyanine (CoPc) was purchased from Sigma Aldrich with 97% purity and used as received. Carbon support (Vulcan XC-72) was purchased from Cabot Corporation, and pyridine (Py) was purchased from Sinapharm Chemical Reagent Co., Ltd. Py-CoPc/C catalysts were prepared from a mixture precursor containing 40 wt% of CoPc + Py and 60 wt% of carbon, where the mass ratio of CoPc and Py was 1:1. For the solid-state reaction, the formed precursor mixture above was dispersed in 10 mL methanol solvent, milled in a mortar for 2 hours, then dried in a vacuum at 40^{o}C for 1 hour to form a powder. The resulting powder was then thermally treated in an N_2 atmosphere from 600^{o}C – 900^{o}C for 2 hours at the rate of 5^{o}C min^{-1}. For a better comparison, three baseline samples of carbon loaded with Py, Py-Co and pure CoPc were also prepared under the same conditions described above.

2.2 Catalyst physical characterization

For physical characterization of the samples, the XRD patterns in the 2θ range from 5^{o} to 90^{o} were performed on a Philips PW3830 X-ray diffractometer using Cu-kα radiation (λ=0.15406 nm).The current was 40 mA and the voltage was 40 KV. XPS analysis was carried out with a Kratos AXIS Ultra^{DLD} electron spectrometer to determine the surface composition with Al K X-ray anode source (hν = 1486.6 eV) at 250 W and 14.0 kV. TEM images were also taken by a JEM-2100F (Hita-chi) at 200 kV to obtain information of the average particle size and the distribution of the catalyst prepared.

2.3. Electrode measurements

For working electrode preparation, a pre-cleaned rotating disk electrode (RDE) (glassy carbon electrode (GC) with a disk diameter of 6.0 mm corresponding to a geometric surface area of 0.283 cm^2, purchased from Pine Instruments) was coated with catalyst to form the catalyst layer. The catalyst ink for this purpose was prepared by mixing 4.0 mg catalyst with 2.0 mL of isopropyl alcohol, which was ultrasonically dispersed for 10 minutes to form a suspension. Then 10 μL of this suspension was pipetted onto the surface of GC electrode and then dried at room temperature. After drying, one drop of methanol/Nafion® solution (50:1 wt%) was then deposited onto the top of the catalyst layer to protect the catalyst from falling off during the electrochemical measurements. The overall catalyst loading was 70.6 μg cm^{-2}.

RDE (Pine, 5908Triangle Drive, Raleigh, NC) measurements were performed in a standard three-compartment electrochemical cell at 25°C. The catalyst coated GC electrode was used as the working electrode. A Pt wire and a saturated calomel electrode (SCE) were used as the counter and reference electrode, respectively. All measured potentials were converted into the values referring to a standard hydrogen electrode (SHE). Electrochemical experiments were carried out in 0.1M KOH solution. For CVs, the electrode was scanned at a scan rate of 50 mV s^{-1} in the potential range between −0.30 and 0.60 V to measure the surface behavior of the catalyst in N_2-saturated KOH solution, and the ORR activity of the catalyst in O_2-saturated 0.1 M KOH solution, respectively. For more quantitative measurements of ORR activity, LSV was conducted on the catalyst-coated RDE in the potential range between −0.35 and 0.2 V in O_2-saturated 0.1 M KOH solution at various rates of rotation. In order to ensure a steady state in each point of the curve, a slow sweeping rate of 5 mV s^{-1} was applied. All electrochemical measurements were performed using a potentiostat (CHI 760 electrochemical analyzer) at ambient conditions.

3. RESULT AND DISCUSSION

3.1 ORR activity of the catalysts

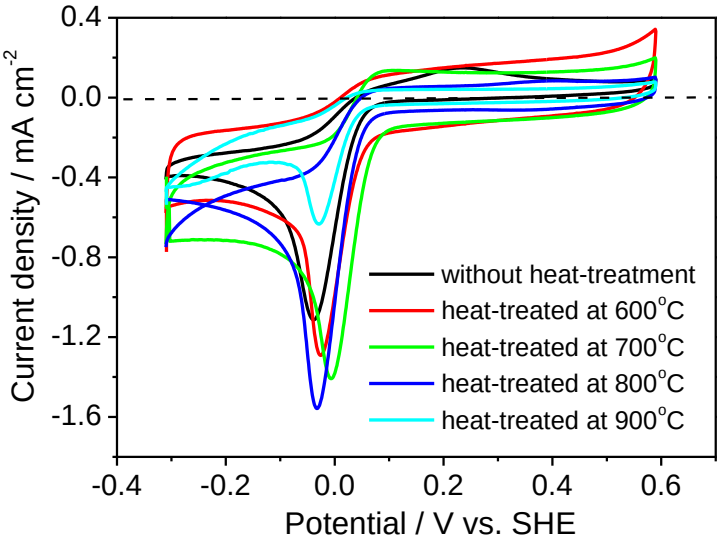

Figure 1. Cyclic voltammograms of a glass carbon disk electrode (0.283 cm^2) coated by several Py-CoPc/C catalysts (heat-treatment temperatures are as marked in the figure), respectively, recorded in O_2-saturated 0.1 M KOH solution at room temperature. Potential scan rate: 50 mV·s^{-1}, and catalyst loading: 70.6 μg cm^{-2}.

For ORR activity of the synthesized catalysts, Fig. 1 shows the CVs of the Py-CoPc/C (the composition of this catalyst is: 20 wt% of Py, 20 wt% of CoPc, and 60 wt% of carbon) samples without and with heat-treatment at 600, 700, 800 and 900°C, respectively, recorded under saturated O_2

atmosphere in 0.1 M KOH solution. As can be seen in Fig. 1, the oxygen reduction peaks can be observed for all of the Py-CoPc/C catalysts, suggesting that these catalysts all have ORR activity regardless of whether they are heat-treated or not heat-treated. As summarized in Table 1, we can see that both Py-CoPc/C catalysts heat-treated at 700 and 800^{o}C show higher ORR activities than that of unpyrolyzed catalyst, if both their onset potentials and the peak potentials are compared. This is consistent with the common belief that heat-treatment can effectively improve the catalytic ORR activity of catalysts [17-24]. In terms of the heat-treatment temperature, 700^{o}C seems to be optimal for heat-treatment, suggesting that the Py-CoPc/C catalyst under heat-treatment at 700^{o}C may provide the most active sites for the ORR.

Table 1. Comparison of electrochemical data of Py-CoPc/C catalysts without and with heat-treatment at different temperatures and, those of CoPc/C, Py-Co/C and Py/C catalysts.

Temperature (^{o}C)	E_p (mV)	Diffusion Limiting current density (mA / cm^2)	Half-wave potential (V)	Onset-potential (V)	n @ -0.35V K–L plot
Py-CoPc/C without heat-treatment	-33	2.94	-0.03	0.19	2.38
Py-CoPc/C-600^{o}C	-25	2.68	-0.02	0.11	2.47
Py-CoPc/C-700 ^{o}C	0	3.29	0.03	0.24	3.08
Py-CoPc/C-800 ^{o}C	-25	3.48	-0.01	0.24	3.05
Py-CoPc/C-900 ^{o}C	-35	1.6	-0.1	0.05	1.91
CoPc/C-700 ^{o}C	-37	2.43	-0.03	0.07	2.05
Py-Co/C-700^{o}C	-129	3.04	-0.11	0.06	2.95
Py/C-700 ^{o}C	-243	1.71	-0.19	-0.05	1.64

For further clarifying the effect of heat-treatment temperature on the ORR activity, LSV was conducted on Py-CoPc/C electrodes in an O_2-saturated 0.1 M KOH solution. As show in Fig. 2(A), the catalyst obtained by heat-treatment at 700^{o}C again shows the highest ORR activity among the catalysts studied. As summarized in Table 1, the ORR half-wave potential for the catalyst heat-treated at 700^{o}C is 30 mV, which is ~ 60 mV higher than that of Py-CoPc/C catalyst without heat-treatment. In addition, the diffusion-limiting currents for the Py-CoPc/C heat-treatment at 700 and 800^{o}C catalysts are also higher than that without heat-treatment, indicating that the ORR overall electron transfer number of the former is more than the latter. Further from Fig. 2(A), it can be seen that with increasing heat-treatment temperature, the ORR activity keeps increasing up to 700^{o}C, then starts to decrease with additional increasing the heat-treatment temperature, suggesting that ~700^{o}C may be the optimal heat-treatment temperature in obtaining the most electroactive catalyst. In other words, more Co-N_X-C active sites could be produced with increasing heat-treatment temperature below 700^{o}C. However,

when temperature is further increased to that higher than 800°C such as at 900°C, the undesired formation of mainly Co and Co oxide (as detected later in XRD experiments) will occur, leading to a reduced concentration of Co-N_X-C moieties on the catalyst surface.

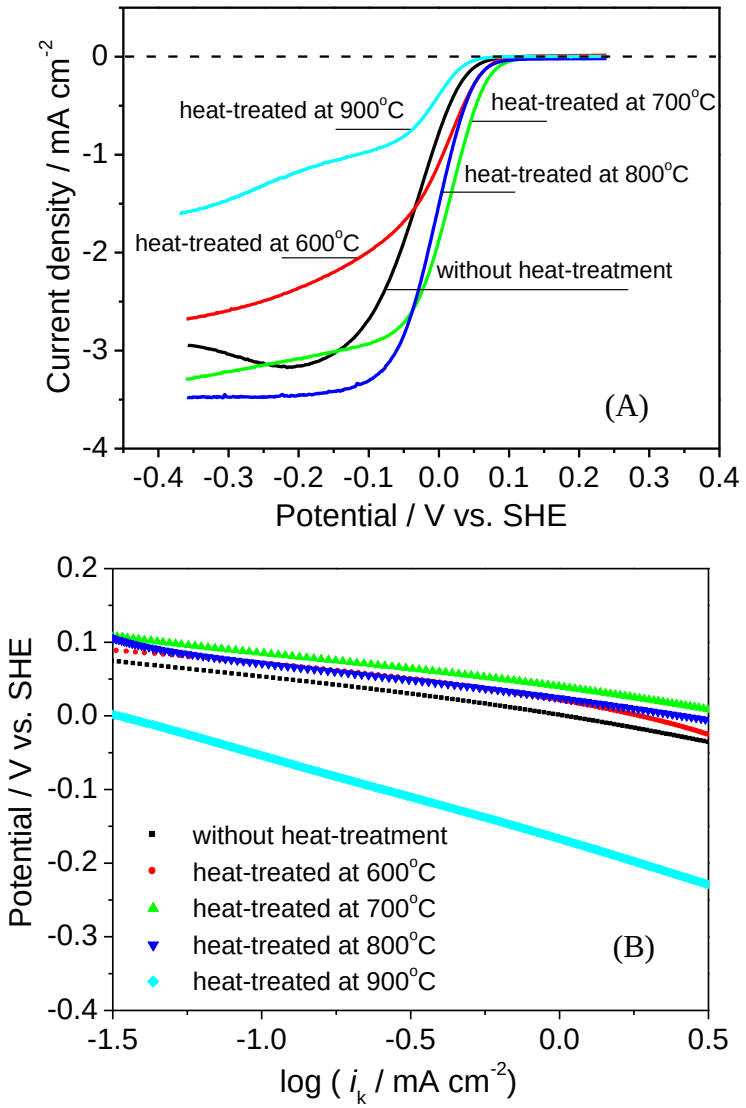

Figure 2. (A) Current-voltage curves of a glass carbon disk electrode (0.283 cm^2) coated by several Py-CoPc/C catalysts (heat-treatment temperatures are as marked in the figure), respectively, recorded at an electrode rotating rate of 1500 rpm in O_2-saturated 0.1 M KOH solution at room temperature. Potential scan rate: 5 $mV \cdot s^{-1}$, and catalyst loading: 70.6 μg cm^{-2}. (B) Tafel plots of E vs. $\log(\frac{i_d i_l}{i_l - i_d})$, data from (A).

Fig. 2(B) presents the mass-corrected Tafel plots of log j_k (mA cm^{-2}) *vs.* the electrode potential E for the ORR on the Py-Co-Pc/C catalysts treated at different temperatures, measured in an O_2-saturated 0.1 MKOH solution. These Tafel curves were deduced from the polarization curves of Fig. 2(A) with an electrode rotation rate of 1500 rpm. The Tafel equation can be expressed as:

$$E = a + \frac{RT}{\alpha n_\alpha F}\log(\frac{i_d i_l}{i_l - i_d}) \quad (1)$$

Where a is the ORR exchange current density related constant, n_α is the charge transfer number in the reaction rate determining step of the catalyzed ORR, α is the n_α associated charge transfer coefficient, i_d is the disk current density, i_l is the diffusion limiting current density, R is the universal gas constant, and T is the temperature.The Tafel slope ($b = \frac{RT}{\alpha n_\alpha F}$) is the parameter measuring the electrode potential change with increasing current density, that is, the larger the b value, the more the electrode potential drop with increasing current density. If assuming the charge transfer number (n_α) in the reaction rate determining step of the catalyzed ORR is 1, the charge transfer coefficient (α) can be calculated based on the equation of $b = \frac{RT}{\alpha n_\alpha F}$.

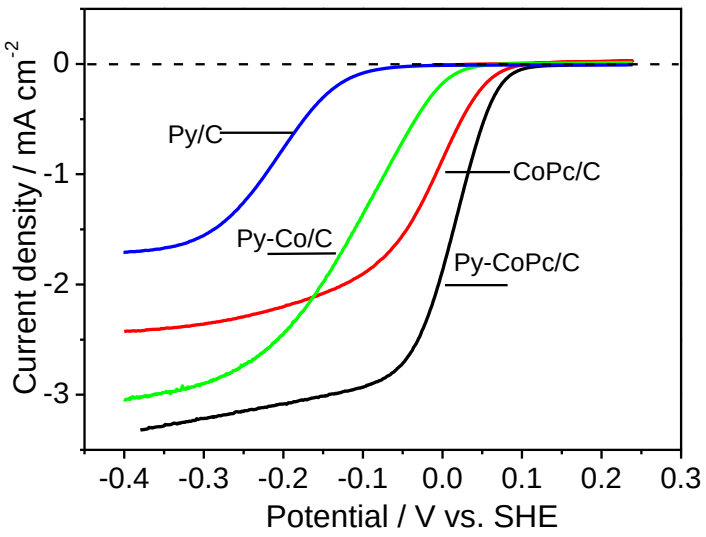

Figure 3. Current-voltage curves of a glass carbon disk electrode (0.283 cm^2) coated by four different catalysts (Py/C, Py-Co/C, CoPc/C and Py-CoPc/C), respectively, recorded at an electrode rotating rate of 1500 rpm in O_2-saturated 0.1 M KOH solution at room temperature. Potential scan rate: 5 mV·s^{-1}, and catalyst loading: 70.6 μg cm^{-2}.

For the case shown in Fig. 2(B), the Tafel slopes for Py-CoPc/C without and with heat-treatment at 600, 700, 800 and 900^{o}C are calculated to be 71, 70, 62, 68 and 111 mV dec^{-1}, respectively. Thus, the calculated values of α are 0.83, 0.84, 0.95, 0.87, and 0.53, respectively, suggesting that Py-CoPc/C heat-treated at 700 ^{o}C is the most active catalyst among these five catalysts.Regarding the additive effect of pyridine into the CoPc catalyst, the ORR result for 40%CoPc/C catalyst was also presented, and compared to that of 40%(Py-CoPc)/C catalyst heat-treated at 700^{o}C. Fig. 3 shows the polarization curves for oxygen reduction catalyzed by Py/C, Py-Co/C, CoPc/C and Py-CoPc/C in O_2-saturated 0.1 mol L^{-1} KOH solution. It can be clearly seen that Py-CoPc/C shows the most ORR activity in all catalyst samples tested, where the ORR half-wave potential of Py-CoPc/C catalyst is positively shifted by 220 mV, 60 mV and 41 mV, respectively, compared to that of Py/C, CoPc/C and Py-Co/C catalysts. In addition, the ORR diffusion current density catalyzed by Py-CoPc/C catalyst is 106%, 40% and 17% higher than that catalyzed by Py/C, CoPc/C and Py-Co/C catalysts, suggesting that the overall ORR electron transfer number of the former is more than that catalyzed by the latters. Therefore, using Py to modify the CoPc can significantly increase the Co-N_X-C active sites, and then improve the catalytic ORR activity.

For a more quantitative estimation of the overall ORR transfer numbers catalyzed by different catalysts, the RDE measurements were also carried out at different electrode rotating rates using all catalysts synthesized in this paper. As an example, Fig. 4 shows one set of current-voltage curves using the optimal catalyst of Py-CoPc/C treated at 700^{o}C. It can be seen from Fig 4(A) that the limiting current density increases with increasing rotation rate, while the on-set potential for the ORR remains unchanged. The transferred electron number per oxygen molecule involved in the oxygen reduction at Py-CoPc/C electrode can be determined by the Koutecky-Levich equation given below [25]:

$$i_d = \left(\frac{1}{i_k} + \frac{1}{i_f} + \frac{1}{i_l} \right)^{-1} \qquad (2)$$

Where i_k is the ORR kinetic current density, i_f is the O_2 diffusion current density through the ionomer in the electrode coating layer, and i_l is the limiting current density induced by O_2 diffusion from solution through catalyst layer. Our calculation based on the ionomer used in the catalyst layer showed that this i_f is much higher than both those i_d and i_k, therefore, its reciprocal can be negligible. In this case, Equation (2) can be simplified to:

$$i_d = \left(\frac{1}{i_k} + \frac{1}{i_l} \right)^{-1} \qquad (3)$$

The i_l can be expressed as:

$$i_l = 0.201nFC_{O_2}D_{O_2}^{2/3}\gamma^{-1/6}\omega^{1/2} \quad (4)$$

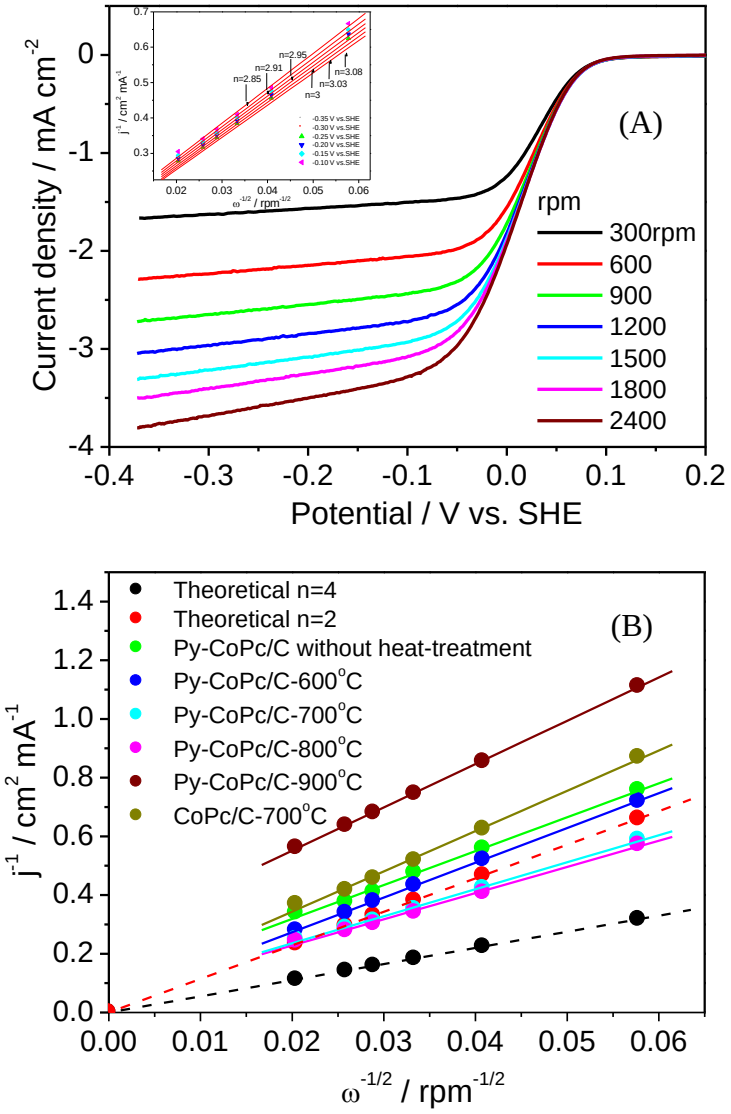

Figure 4. (A) Current-voltage curves of a glass carbon disk electrode (0.283 cm^2) coated by Py-CoPc/C heat-treated at 700°C, recorded at different electrode rotating rates from 300 to 2400 rpm in O_2-saturated 0.1 M KOH solution at room temperature. Potential scan rate: 5 mV s^{-1}, and catalyst loading: 70.6 μg cm^{-2} (Insert: Koutecky–Levich plots at different electrode potential). (B) Koutecky–Levich plots for different catalysts as marked in the figure, other conditions are the same as in (A).

Where n is the ORR overall electron transfer number, F is the Faraday's constant (96485 C mol^{-1}), C_{O_2} is the concentration (or solubility) of O_2 in the electrolyte solution (mol cm^{-3}), R is the universal gas constant (8.314 J mol^{-1} K^{-1}), D_{O_2} is the diffusion coefficient of O_2 (cm^2 s^{-1}), γ is the kinematic viscosity of the KOH aqueous solution (cm^2 s^{-1}), and ω is the electrode rotating rate (rpm). In this Equation (4), any reduction in the value of C_{O_2} or D_{O_2}, or any increase in γ can cause the decrease in diffusion limited current density.

The inset in Fig. 4(A) shows the Koutecky-Levich plots of Py-CoPc/C heat-treated at 700^{o}C at -0.35, -0.3, -0.25, -0.2, -0.15 and -0.1 V, respectively. From the slopes of the plots, the overall ORR electron transfer numbers can be calculated, which are 2.85, 2.91, 2.95, 3.00, 3.03 and 3.08, respectively. The average value is 2.97, suggesting that the catalyzed ORR is a 3-electron transfer process through a 2 + 2 electron transfer mechanism: one is the 2-electron reduction of O_2 to HO_2^-, then followed by the further 2-electron reduction of HO_2^- to OH^-. Due to the produced HO_2^- might be only partially further reduced on the electrode surface through a 2-electron transfer pathway, the apparent overall electron transfer number is less than 4 in this case.

Fig. 4(B) shows the Koutecky–Levich plots at -0.35 V vs. SHE for the ORR on catalyzed by all catalysts studied in this paper for comparison. For a better comparison, the theoretical plots for the 2-electron and 4-electron transfer processes of the ORR are also shown in Fig. 4(B). According to the slopes of these plots measured under the same experiment conditions, the obtained overall ORR electron transfer numbers for three typical catalysts, ie., Py-CoPc/C and CoPc/C heat-treated at 700^{o}C and Py-CoPc/C without heat-treatment are 3.08, 2.05 and 2.38, respectively, suggesting that the Py-CoPc/C catalyst heat-treated at 700^{o}C has the most overall ORR electron number.

3.2. Physical characterization of the catalysts for understanding the ORR activity

To study the crystal structure and the composition of the synthesized catalysts, and understand their catalytic ORR activity, both Py-CoPc/C samples without and with heat-treatment at different temperatures were investigated by XRD measurements. Fig. 5 shows the XRD patterns of the catalysts synthesized without and with heat-treatment at 600, 700, 800 and 900^{o}C, respectively. The broad signal centered at 24.7^o corresponds to the diffraction of graphitic carbon and, the intensity of this graphite peak becomes strong and narrow with increasing heat-treatment temperature, indicating that the graphitization of the macrocycle increases with increasing heat-treatment temperature. In the case of Py-CoPc/C without heat-treatment, all peaks of CoPc (6.86^o and 9.64^o) and XC-72 carbon powder (24.7^o) can be clearly seen. Comparing heat-treated catalysts to that without heat-treatment, it can be observed that several characteristic diffraction peaks disappear after heat-treatment, such as the characteristic peaks of CoPc at 6.86^o and 9.64^o and its other characteristic peaks also becomes weak. Lalande et al. [20,23] observed that the nature of the catalytic site was dependent on the heat-treatment temperature, and described the processes induced by heat-treatment as: (1) ~400^{o}C: dehydration; (2)

400 – 600^{o}C: completion of the polymerization reaction during which Co-phthalocyanine polymer was stable up in this temperature range; (3) 600 – 800^{o}C: pyrolysis of the polymer to produce fragments containing Co bound to C and N on the catalyst surface and Co-N_X-C active sites were produced; (4) Above 800^{o}C: inorganic Co (Co^{o} and Co(II)) and Co oxide could be produced on the support. The observation from the XRD analysis in Fig. 5 is in a good agreement with above four steps.

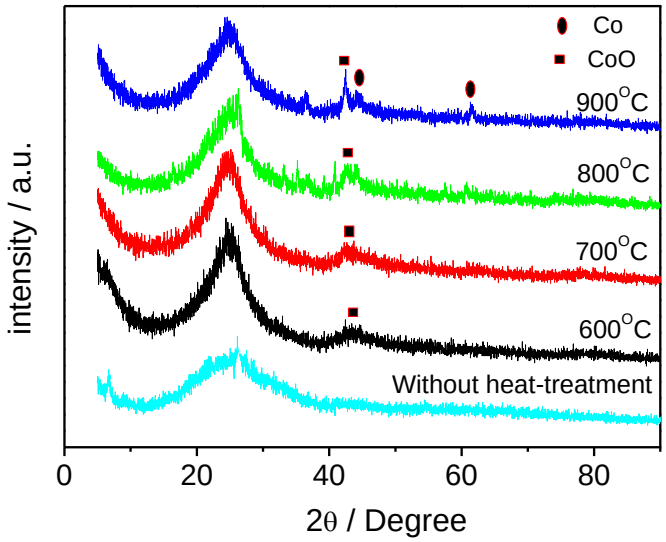

Figure 5. XRD patterns of Py-CoPc/C catalysts heat-treated at different temperatures.

It can be seen that after heat-treatment at 900^{o}C, three diffraction peaks centered at 42^{o}, 43.3^{o} and 61^{o}, respectively, can be observed, which indicates that part of the Py-CoPc/C on the carbon support probably have been decomposed, forming new compositions. According to literatures [26-28], these two diffraction peaks may correspond to the characteristic diffraction peaks of Co and Co oxides. For samples heat-treated at 900^{o}C, these peaks are slightly taller than that of heat-treated at 800^{o}C, indicating the structure of Co-N_X-C might be destroyed.

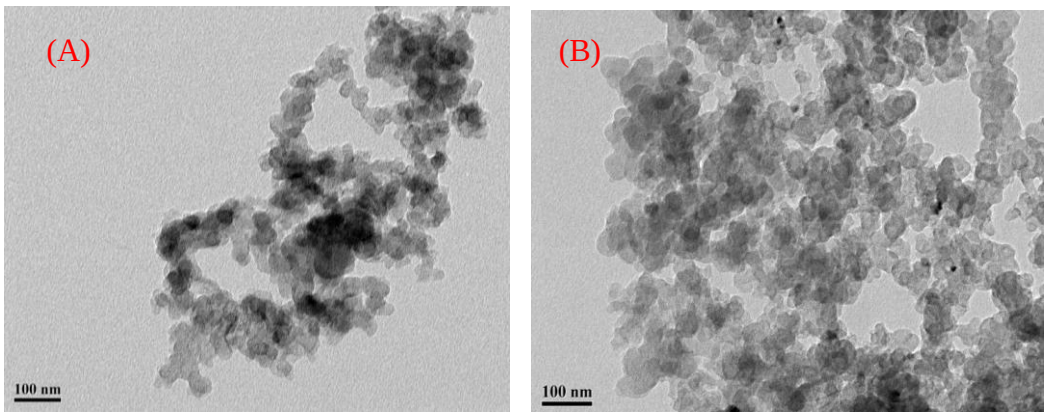

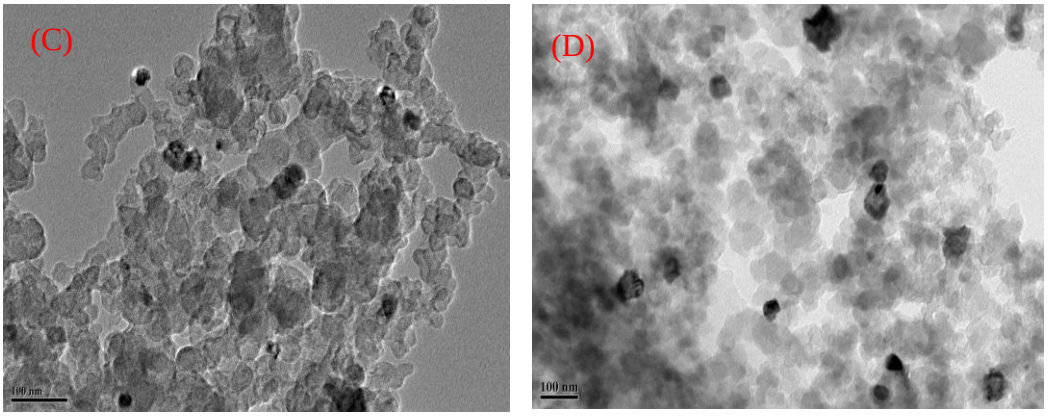

Figure 6. TEM images of Py-CoPc/C catalysts heat-treated at (A) 600°C, (B) 700°C, (C) 800°C, and (D) 900°C, respectively.

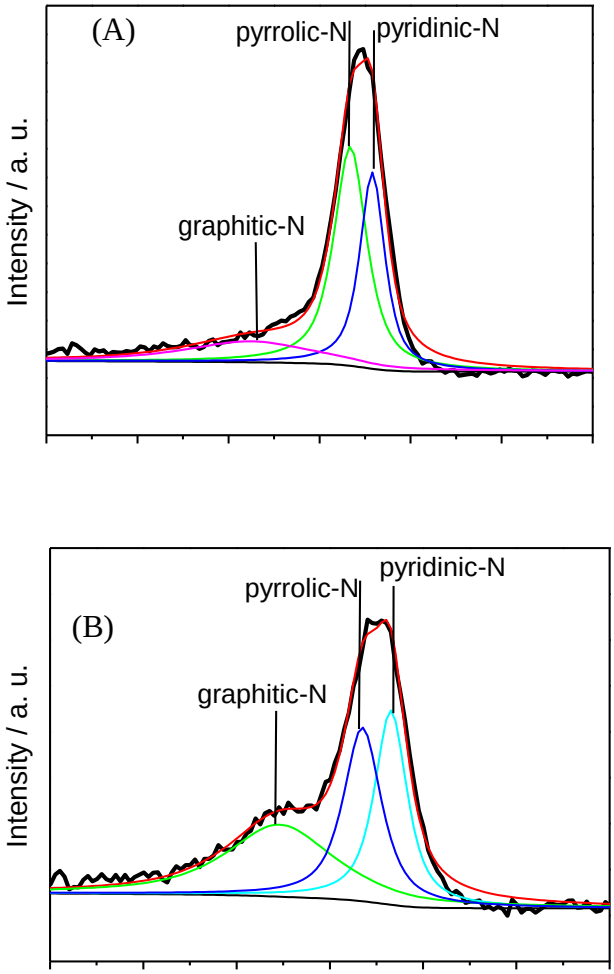

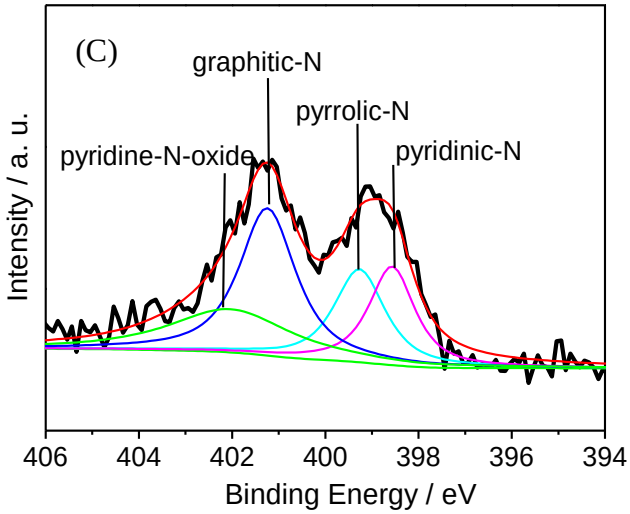

Figure 7. XPS N1 spectra of Py-CoPc/C catalysts (A) without heat-treatment, (B) heat-treated at 700^{o}C, and (C) heat-treated at 900^{o}C, respectively.

For morphology of the synthesized catalysts, TEM images were taken after heat-treatment at 600, 700, 800 and 900^{o}C, respectively, as shown in Fig. 6. It can be seen that the TEM image of Py-CoPc/C catalyst heat-treated at 600^{o}C shows a slightly agglomeration of the nanosized particles (Fig. 6(A)). When the Py-CoPc/C samples was heat-treated at 700^{o}C, the resulting particles exhibit an average size of about 20 nm with a uniform dispersion on the Vulcan XC-72 support (Fig. 6(B)). As indicated by XRD in Fig. 5 and literature [16-24], the formed materials in temperature range of 700-800^{o}C should be Co-N_X-C sites residing on the carbon surface. These Co-N_X-C sites are responsible for the catalytic ORR activity.With increasing temperature to 800^{o}C, some small and very diluting metal particles (black dots) are appeared, but the sample still has a uniform dispersion (Fig. 6(C)). This result indicates that part of Co-N_X-C sites is converted into metal particles. However, when the temperature is further increased to 900^{o}C, some large particles (black dots) can be observed and the crystalline particles have an average size of about 50 nm, surrounded by a shell of carbon layer (Fig. 6(D)). These particles could be attributed to the metal Co phase aggregated on the carbon support surface although the metal particles are encapsulated within the carbon substrates [29-31]. These results suggest that heat-treatment at temperature higher than 800^{o}C can decompose the Co-N_X-C structure to metallic Co, which then agglomerates into large particle size when further increasing the heat-treatment temperature. This result is consistent with the observation from the XRD analysis in Fig. 5. It is generally recognized that this metal Co phase is not active towards ORR [20,32]. Due to the decomposition of ORR active site (Co-N_X-C), its concentration would become smaller, leading to the drop of ORR activity when the heat-treatment temperature is higher than 800^{o}C, as observed in ORR measurements (Fig. 2).

In order to further detect the chemical state of surface catalyst particles before and after the heat-treatment, Fig. 7 presents the XPS survey spectra of Py-CoPc/C catalysts without and with heat-treatment at 700 and 900 ^{o}C, respectively. Based on literatures [29,33,34], the peaks of N1s at 398.6 eV, 399.9 eV, 401.2eV and 402.2 eV can be assigned to the pyridinic-N, pyrrolic-N, graphitic-N and pyridine-N-oxide, respectively. Among these peaks of N1s, pyridinic-N and graphitic-N are believed to play important roles in the ORR active sites of the catalyst. On the other hand, pyridine-N-oxide seems useless in improving the ORR activity [30,35]. As shown in Fig. 7(A), three different nitrogen states can be observed for the non-heat-treated catalyst sample, which correspond to pyridinic-N (398.6 eV), pyrrolic-N (399.9 eV) and graphitic-N (401.2 eV). As shown in Fig. 7(B), the similar situation occurs when the sample was heat-treated at 700^{o}C. However, pyridinic-N and graphitic-N at 700^{o}C are largely increased compared to that of non-heat-treated sample. The dominant peak at 398.6 eV present in the spectra suggests that pyridinic-N is the major state in the N1s, which should be responsible for the high electrocatalytic ORR activity. This is why we observed that the Py-CoPc/C catalyst heat-treated at 700^{o}C gives a higher activity than the Py-CoPc/C catalyst without heat-treatment, as tested in the sections above. After the sample was heat-treated at 900^{o}C, the N1s peak is disassembled into four components: 398.60, 399.9, 401.2 and 402 eV, respectively, which can be attributed to pyridinic-N, pyrrolic-N, graphitic-N and pyridine-N-oxide, respectively. Compared to the Py-CoPc/C sample heat-treated at 700^{o}C, the difference is that the pyridine-N-oxide can be observed and a notable fall of the magnitude of the pyridinic-N. These may at least partially explain the result that the electrocatalytic activity was decreased dramatically after the catalyst was heat-treated at 900^{o}C, as shown in Fig. 2. It also can be seen from Fig. 7(B), graphitic-N content is greatly increased after the sample is heat-treated at 700^{o}C. According to literatures [36,37], graphitic-N could catalyze the ORR through a 4-electron transfer pathway. Therefore, it can be concluded that both pyridinic-N and graphitic-N should mainly responsible for the enhanced ORR activity on Py-CoPc/C catalysts.

4. CONCLUSIONS

The carbon-supported non-precious metal (Co) catalysts, namely Py-CoPc/C, were synthesized using combined solvent-impregnation and milling procedures along with the high-temperature treatment. For heat-treatment effect on the catalysts activity, the catalyst precursor was heat-treated at 600, 700, 800, and 900^{o}C, respectively, and the resulting catalysts were tested using both CV and RDE techniques in O_2-saturated 0.1M KOH solution for the catalytic activity toward oxygen reduction reaction. All heat-treated catalysts showed ORR activities with the one at 700^{o}C heat-treatment giving the best activity, which is indicated by both the ORR onset potential of 0.24 V vs. SHE and a half-wave potential of 0.03 V. Therefore, for Py-CoPc/C catalysts, heat-treatment temperature of 700^{o}C should be the optimal temperature.

For pyridine addition effect on the CoPc/C catalyst, pyridine was added into the CoPc/C precursor and ball-milled to form the catalysts. The formed Py-CoPc/C catalysts all showed the better ORR activities than that CoPc/C catalyst alone, indicated by both the higher onset (or half-wave) potential and the more overall ORR electron transfer number. Therefore, using pyridine to modify the CoPc can significantly increase the number of Co-N_X-C active sites, and then improve the catalytic ORR activity.

To understand both the heat-treatment and pyridine addition effects on the catalytic ORR activity of the synthesized Py-CoPc/C catalysts, XRD, TEM as well as XPS were employed to study the crystal structures, morphologies and surface structure changes. Both XRD and TEM analysis indicated that the structure of Py-CoPc/C was decomposed after heat-treatment, forming the Co-N_X-C active sites, which is responsible for the ORR. When heat-treatment temperature was lower than 700^{o}C, the amount of Co-N_X-C active sites was increased, leading to an enhanced catalytic activity. However, when the temperature was higher than 700^{o}C, the Co-N_X-C active sites were partially decomposed to form both metal Co and Co oxides, resulting in a drop in catalytic activity. XPS results suggested that the pyridinic-N and graphitic-N groups might be responsible for the enhanced ORR activity, and the catalyst formed at 700^{o}C treatment showed the most amount of these two groups, leading to the most active ORR catalyst.

ACKNOWLEDGMENTS

This work was supported by the National Natural Science Foundation of China (21173039); Specialized Research Fund for the Doctoral Program of Higher Education, SRFD (20110075110001) of China; State Environmental Protection Engineering Center for Pollution Treatment and Control in Textile Industry of China, and opening Foundation of Zhejing Provincial Top Key Discipline, China (20110927). All the financial supports are gratefully acknowledged.

References

1. L. Zhang, J.J. Zhang, D.P. Wilkinson, H.J. Wang, *J. Power Source* 156 (2006) 171.
2. J. Prakash, D. Tryk, A.W. Aldred, E.B. Yeager, *J. Appl. Electrochem.* 29 (1999) 1463.
3. J.H. Kim, A. Ishihara, S. Mitsushima N. Kamiya, K.I. Ota, *Electrochim. Acta* 52 (2007) 2492.
4. K.C. Lee, A. Ishihara, S. Mitsushima, N. Kamiya, K.I. Ota, *Electrochim. Acta* 49 (2004) 3479.
5. H.S. Liu, C.J. Song, Y.H. Tang, J.L. Zhang, J.J. Zhang, *Electrochim. Acta* 25 (2007) 4532.
6. F.Y. Cheng, *J. Chem Soc. Rev.* 41 (2012) 2172.
7. M. Isaacs, M.J. Aguirre, A. Toro-Labbe, J. Costamagna, M. Pa ´ez, J.H. Zagal, *Electrochim. Acta* 43 (1998) 1821.
8. Z.W. Chen, D. Higgins, A. Yu, L. Zhang, J.J. Zhang, *Energy Environ Sci* 4 (2011) 3167.
9. X.G. Li, C.P. Liu, W. Xing, T.H. Lu, *J. Power Sources* 193 (2009) 470.
10. A. Morozan, B. Jousselme, S. Palacin, *Energy Environ Sci* 4 (2011) 1238.
11. K. Essaki, E.J. Rees, G.T. Burstein, G.E. Haslam, *ECS Trans* 25 (2009) 141.
12. M. Lefe `vre, J.P. Dodelet, *Electrochim. Acta* 48 (2003) 2749.
13. R. Baker, D.P. Wilkinson, J.J. Zhang, *Electrochim. Acta* 53 (2008) 6906.

14. Z.W. Xu, H.J. Li, G.X. Cao, Q.L. Zhang, K.Z. Li, X.N. Zhao, *J. Mol. Catal. A* Chem 335 (2011) 89.
15. R. Jasinski, *Nature* 201 (1964) 1212.
16. M. Lefe ´vre, E. Proietti, F. Jaouen, J.P. Dodelet, *Science* 324 (2009) 71.
17. G. Faubert, R. Cote, D. Guay, J.P. Dodelet, G. Denes, P. Bertrandc, *Electrochim. Acta* 43 (1998) 341.
18. H.T. Chung, C.M. Johnston, P. Zelenay, *ECS Transactions* 25 (2009) 485.
19. R. Cote, G.T. Lalande, L.D. Bailey, D. Guay, J.P. Dodelet, *J. Electrochem. Soc* 145 (1998) 2411.
20. G. Lalande, R. CôTé, G. Tamizhmani, D. Guay, J.P. Dodelet, L. Dignard-Bailey, L.T. Weng, P. Bertrand, *Electrochim. Acta* 40 (1995) 2635.
21. Y. Nabae, S. Moriya, K. Matsubayashi, S.M. Lyth, M. Malon, L. Wu, *Carbon 48* (2010) 2613.
22. L.C. Wang, L. Zhang, J.J. Zhang, *Electrochim. Acta*, 56, 5488-5492 (2011)]
23. C.W.B. Bezerra, L. Zhang, K.C. Lee, H. Liu. A.L.B. Marques, E.P. Marques, H.J. Wang, J.J. Zhang, *Electrochim. Acta* 53 (2008) 4937.
24. C.W.B. Bezerra, L. Zhang, K. Lee, H. Liu, J. Zhang, Z. Shi, A.L.B. Marques, E.P. Marques, S. Wu, J.J. Zhang, *Electrochim. Acta* 53 (2008) 7703.
25. J. Bard, L. Faulkner, Electrochemical Methods, 2nd ed., *Wiley & Sons*, NJ, p 331.
26. H. Zhu, X.W. Li, F.H. Wang, *Int. J. Hydrogen. Energy* 36 (2011) 9151.
27. A. Sarkar, A. Manthiram, *J. Phys. Chem. C* 114 (2010) 4725.
28. R.F. Wang, H. Li, H.Q. Feng, H. Wang, Z.Q. Lei, *J. Power Sources* 195 (2010) 1099.
29. V. Nallathambi, J.W. Lee, S.P. Kumaraguru, G. Wu, N.B. PoPov, *J. Power Sources* 183 (2008) 34.
30. G. Liu, X.G. Li, P. Ganesan, N, B. Popov, *Electrochim. Acta* 55 (2010) 2853.
31. G. Liu, X.G. Li, P. Ganesan, B.N. Popov, *Appl. Catal. B: Environ.* 93 (2009) 156.
32. T. Okada, M. Gokita, M. Yuasa, I. Sekine, *J. Electrochem. Soc.* 145 (1998) 815.
33. X.G. Li, G. Liu, N. Popov, *J. Power Sources* 195 (2010) 6373.
34. K.C. Lee, L. Zhang, H.S. Liu, R. Hui, Z. Shi, J.J. Zhang, *Electrochim. Acta* 54 (2009) 4704.
35. A. Velázquez-Palenzuela, L. Zhang, L.C. Wang, P.L. Cabot, E. Brillas, K. Tsay, *J. Phys. Chem. C* 115 (2011) 12929.
36. H. Niwa, K. Horiba, Y. Harada, M. Oshima, T. Ikeda, K. Terakura, *J. Power Sources* 187 (2009) 93.
37. A.R. Sidik, B.A. Anderson, P.N. Subramanian, P.S. Kumaraguru, N.B. Popov, *J. Phys. Chem. C* 110 (2006) 1787.